ISH Journal of Hydraulic Engineering

ISSN: (Print) (Online) Journal homepage: https://www.tandfonline.com/loi/tish20

Coupling wavelet transform with multivariate adaptive regression spline for simulating suspended sediment load: Independent testing approach

Naser Shiri , Jalal Shiri , Vahid Nourani & Sepideh Karimi

To cite this article: Naser Shiri , Jalal Shiri , Vahid Nourani & Sepideh Karimi (2020): Coupling wavelet transform with multivariate adaptive regression spline for simulating suspended sediment load: Independent testing approach, ISH Journal of Hydraulic Engineering, DOI: 10.1080/09715010.2020.1801528

To link to this article: https://doi.org/10.1080/09715010.2020.1801528

Published online: 04 Aug 2020.

ISH JOURNAL OF HYDRAULIC ENGINEERING
https://doi.org/10.1080/09715010.2020.1801528

Taylor & Francis
Taylor & Francis Group

Coupling wavelet transform with multivariate adaptive regression spline for simulating suspended sediment load: Independent testing approach

Naser Shiri[a], Jalal Shiri[b,c], Vahid Nourani[a,c] and Sepideh Karimi[a]

[a]Faculty of Civil Engineering, University of Tabriz, Tabriz, Iran; [b]Water Engineering Department, Faculty of Agriculture, University of Tabriz, Tabriz, Iran; [c]Center of Excellence in Hydroinformatics, Faculty of Civil Eng., University of Tabriz, Tabriz, Iran

ABSTRACT

Accurate prediction of suspended sediment load (SSL) of a river is very important as it directly affects the performance of the corresponding hydraulic structures. SSL can give valuable information on the catchment erodibility and deposition of the sediment being produced through scouring phenomenon. Despite the hydraulic approaches for studying the scouring/sedimentation processes in streams, hydrologic approaches may provide valuable information about SSL deposition magnitudes as well as its temporal distribution in relation with the streamflow power. A hydrologic-based approach through coupling the wavelet-based processed signals and multi adaptive regression spline (WMARS) methodology is suggested in the present paper for the first time to predict SSL values of rivers using the simultaneous streamflow and SSL records. The developed models were assessed through the most powerful k-fold testing data scanning procedure. The obtained results showed the superiority of the proposed hybrid WMARS models over the single MARS and traditional sediment rating curve techniques. Due to the presence of hysteresis effects during the study periods, adaptation of k-fold testing assessment approach is very necessary to get better insight about the models performances.

ARTICLE HISTORY
Received 9 March 2020
Accepted 23 July 2020

KEYWORDS
K-fold testing; MARS; suspended sediment; wavelet transform

1. Introduction

Accurate estimation of the suspended sediment load (SSL) of a river is of crucial significance in water resources engineering due to its direct impact on the planning, design, management and operation of hydraulic structures. Substantial studies have been carried out so far for developing a universal relationship between the SSL and river flow characteristics in the river, e.g. flow discharge, velocity and the shear stress, although most of them have not been successful in this regard (Vanoni 1971). Those attempts might be classified as physics-based and empirical SSL estimation models. The fundamental of the first group models is on the basis of the simplified partial differential equations of flow and sediment flux. Nonetheless, they employ unrealistic simplifying assumptions for flow and empirical relationships for erosive impacts of the rainfall and streamflow (Aytek and Kisi 2008). The empirical models, on the other hand, try to establish relations between river flow and geometry characteristics with SSL amount (Karim and Kennedy 1990). However, the relations between SSL and river flow are complex due to hysteresis effect and depend on some factors such as: the availability of high-resolution streamflow discharge and sediment concentration data difficulties involved with direct measurement of these variables, and inclusion of the errors of these parameters in SSL estimations (Lopes and Ffolliott 1993; Sivakumar 2006). Nevertheless, establishing such relations needs lots of hydrological data such as distribution of the precipitation (quantitative and qualitative), geologic structure of the catchment region, plant cover, etc (McBean and Al-Nassri 1988). On the other hand, the precipitation shows different effect on SSL magnitude during a year (winter precipitation effect on sediment formation is difficult than the rest of the seasons) that makes the analysis more difficult (Bogardi 1974). Hence, most of the studies have tried to seek relations between the streamflow discharge and SSL. For making relations between river discharge and SSL empirically, regression-based techniques and time series analysis might be good choices, but the former has the limitation of linear relation assumption that is not realistic. So, nonlinear regression-based models, e.g. sediment rating curve (SRC) and multivariate adaptive regression spline (MARS) might be a suitable alternative for traditional regression techniques.

In the recent years, substantial literature has reported the hydrological/hydraulic process modelling including sediment transport process using artificial intelligence models (e.g. Najafzadeh 2020; Najafzadeh and Kargar 2019; Sadeghi et al. 2020; Homaei and Najafzadeh 2020). A complete review of such applications is beyond the scope of the present study and some most relevant studies are reviewed here. Kisi and Shiri (2012) compared different artificial intelligence models in estimating daily SSL values by implicating climatic variables and introduced the genetic programming (GP) as the most robust model in this regard. Kisi et al. (2012) compared GP with support vector machine (SVM) for modelling daily SSL and confirmed the better performance of GP. Atieh et al. (2015) applied integrated neural network (NN) models for estimating the sediment rating curve parameters in ungauged basins. Makarynskyy et al. (2015) coupled the NN with a numerical model for predicting suspended sediment concentration in marine area and approved the proper generalization ability of the NN methods. Ghose and Samantaray (2018) utilized NN and regression methods for predicting minimum sediment concentration values and introduced the NN as capable model in this regard.

CONTACT Naser Shiri nasershiri75@yahoo.com

Samantaray and Ghose (2018) applied discrete neural network in evaluation of suspended sediment concentration and found their acceptable capability in modelling this parameter, although they mentioned the major drawback of giving negative sediment concentration values by this method. Bisoyi et al. (2019) applied a NN method for predicting SSL using data for a period of about 4 years in India and indicated that the developed NN models might be of use in large-scale river systems. Liu et al. (2019) compared the NN and multivariate regression (MLR) in simulating the time frequency and magnitudes of suspended sediment concentration and reported that NN produced more accurate results than the MLR technique.

Although the successful applications of the regression-based and artificial intelligence models for river SSL modelling have been reported in literature, these models failed to give accurate estimations of river system parameters in numerous cases as reported by literature (e.g. Rajaee 2010; Shiri and Kisi 2010; Nourani et al. 2011; Shiri and Kisi 2012; Seo et al. 2016; Khosravi et al. 2018; Graf et al. 2019; Kisi and Yaseen 2019; Tao et al. 2019; Salih et al. 2020). Therefore, substantial attempts have been carried out to improve the performance accuracy of those models using preprocessing techniques, e.g. wavelet analysis. Application of wavelet transforms and their coupling with regression-based and artificial intelligence approaches have been increasing during the recent years in various disciplines of water resources engineering (e.g. Kisi 2009; Wang, 2009; Adamowski and Sun 2010; Peng et al., 2017; Londhe and Narkhdehe 2018; Shiri 2018; Najafzadeh and Zeinolabedini, 2018; Zeinolabedini and Najafzadeh 2019; Zhang et al. 2019). In the context of SSL estimation, various studies have been carried out for testing the capabilities of wavelet-based regression and artificial intelligence models. Among others, Partal and Cigizoglu (2008), Nourani et al. (201), Rajaee (2011) and Nourani et al. (2019) applied a wavelet neural network approach for modelling SSL. Goyal (2014) adopted a wavelet-M5 model for SSL simulation and found that the coupled model gave more accurate results than the neural network model. Himanshu et al. (2017) introduced a wavelet-support vector machine algorithm for modelling SSL using hydro-meteorological data.

The literature review by the authors showed that there is no application of multi-variate adaptive regression spline (MARS) technique and/or coupling it with wavelet for SSL modelling and the adaptation of this method for SSL simulation is presented in this study for the first time for a wide range of SSL and streamflow discharge values. The MARS technique does not need a pre-defined functional relationship between the input and target parameters. Further, it is a non-parametric regression approach that reduces the degree of complexity of a studied phenomenon via making a couple of piecewise linear splines among the independent and dependent variables (Najafzadeh and Oliveto 2020). Therefore, it would be of interest to check its abilities for simulation of SSL values. In spite of that, most of the studies have applied a single data assigning mode where a part of the available patterns has been utilized for training the models or calibrating the sediment rating curves and then, the developed models have been tested/validated using a separate part of the available data. Though this is a common process, the outcomes of such data management scenario would be partially valid because all the available patterns have not been involved in training-testing phases. The present paper, however, used the robust k-fold testing scenario for feeding the applied models with the available input variables.

2. Materials and methods

2.1. Used data

Data from three rivers in USA (obtained from USGS) were used in the presented study for assessing the suggested methodology. Table 1 presents the general information of the studied rivers and stations. The statistical characteristics of the applied sediment and river flow data are summarized in Table 2. Analyzing the statistical characteristics of the data, some remarks can be highlighted. First, the mean SSL values of the Pineville and Barbourville stations are similar (upstream and downstream stations of the Cumberland River), while the average SSL value for the Dos Rios Station is about twice the mean values of the other stations. However, the mean flow discharge values are similar in all three stations. Moreover, the difference between the maximum and minimum SSL values is remarkably large for the Dos Rios Station. Next, the coefficient of variation (C_V) and skewness coefficient values for the SSL records are higher than those of the Q_W in the studied stations that show higher deviations from the mean values for SSL data.

3. Multi-variate adaptive regression spline (MARS)

As a non-parametric regression method, MARS might be considered as a progressive version of linear models that can simulate the interactions between the input and target parameters (Friedman 1991). Its algorithm consists of

Table 1. General information of the studied stations.

River	Station	Station no.	Latitude	Longitude	Data period	Area basin (mile^2)
Cumberland	Barbourville	03403500	36°51′44″	83°53′15″	1979–1989	960
	Pineville	03403000	36°48′48″	83°45′58″	1979–1989	809
Eel	Dos Rios	11,472,150	39°37′30″	123°20′25″	1966–1977	528

Table 2. Statistical characteristics of the applied data.

	Data set	X_{max}	X_{min}	X_{mean}	STDEV	C_v	Skew
Barbourville station	Q_W (m^3/s)	1180	1.44	44.80325	72.00674	1.607177	5.217543
	SSL (mg/day)	165,000	0.13	1187.57	6158.053	5.185425	14.0001
Pineville station	Q_W (m^3/s)	966	1.42	35.70416	58.11106	1.627571	6.395624
	SSL (mg/day)	221,000	0.13	1028.006	6577.347	6.39816	17.94702
Dos Rios station	Q_W (m^3/s)	1590	0	27.24923	84.46966	3.099892	7.508993
	SSL (mg/day)	661,000	0	2156.932	17,643.07	8.179706	19.93401

backward and forward stepwise plans. In the forward stepwise plan, the excessive forward stepwise selection plan builds a complex over-trained model through a number of splits (Andres et al. 2010) that carries less performance accuracy. Hence, the backward stepwise plan eliminates the redundant variables from the previously chosen ones. This function projects X variable to a new Y variable by the following basic functions, employing a variable's knot or value that defines a conjunction point along the range of inputs (Sharda et al. 2006; Adamowski et al., 2012). MARS uses piecewise linear basis functions with the form of $(x\text{-}t)_+$ and $(t\text{-}x)_+$. The suffix '+' illustrates the positive part only. So:

$$(x-t)_+ = \begin{cases} x-t, if x>t \\ 0, otherwise \end{cases} \quad (1)$$

and

$$(t-x)_+ = \begin{cases} t-x, if x<t \\ 0, otherwise \end{cases} \quad (2)$$

The general form of the MARS equation will be:

$$\hat{f}(x) = \sum_{i}^{k} c_i B_i(x) \quad (3)$$

that is indeed a weighted some of $B_i(x)$ function. c_i denotes the constant coefficients identified via minimizing the residual sum of squares (standard linear regression). The coefficients may be assumed as weights which depict the importance of each variable (Shiri 2019).

4. Discrete wavelet transform (DWT)

Wavelet function (mother wavelet) $\psi(t)$ may be expressed as $\int_{-\infty}^{+\infty} \psi(t)dt = 0$.

$\psi_{a,b}(t)$ is identified by compressing and expanding $\psi(t)$ as:

$$\psi_{a,b}(t) = |a|^{-1/2}\psi\left(\frac{t-b}{a}\right) \qquad b\varepsilon R, a\varepsilon R, a\neq 0 \quad (4)$$

$\psi_{a,b}(t)$ is the successive wavelet, a and b show the scale and time factors, respectively; and R shows the real numbers domain.

If $\psi_{a,b}(t)$ satisfies Equation (4), for the time series $f(t) \in L^2$ (R), successive wavelet transform of $f(t)$ will be written as:

$$W_\psi f(a,b) = |a|^{-1/2}\int_R f(t)\ \bar{\psi}\left(\frac{t-b}{a}\right)dt \quad (5)$$

In this equation, $\psi\_(t)$ represents the complex conjugate functions of $\psi(t)$. It is clear from this equation that the wavelet transform is the decomposition of $f(t)$ under different resolution scales.

The successive wavelet is frequently discrete in real applications. Assume $a = a_0^j$, $b = kb_0a_0^j$, $a_0 > 1$, $b_0 \in R$, k, j are integer numbers. Discrete wavelet transform (DWT) of $f(t)$ might be considered as:

$$W_\psi f(j,k) = a_0^{-j/2}\int_R f(t)\ \bar{\psi}\left(a_0^{-j}t - kb_0\right)dt \quad (6)$$

The most common (and simplest) choice for the parameters a_0 and b_0 is 2 and 1 time steps, respectively (Mallat 1989), so Equation (6) will read:

$$W_\psi f(j,k) = 2^{-j/2}\int_R f(t)\ \bar{\psi}\left(2^{-j}t - k\right)dt \quad (7)$$

The characteristics of the original time series in frequency (a or j) and time domain (b or k) at the same time are presented by $W_\psi f(a,b)$ or $W_\psi f(j,k)$.

For a discrete time series $f(t)$, where occurs at different time t (i.e., here integer time steps are used), the DWT would be considered as

$$W_\psi f(j,k) = 2^{-j/2}\sum_{t=0}^{N-1} f(t)\ \bar{\psi}\left(2^{-j}t - k\right) \quad (8)$$

where $W_\psi f(j,k)$denotes the wavelet coefficient for the discrete wavelet of scale $a = 2^j, b = 2^j k$.

DWT operates two sets of functions, e.g. high-pass and low-pass filters. The original time series are passed through these filters and separated at different levels. The time series is decomposed into one comprising its trend which is the outcome of the low-pass filter (high-scale and low-frequency wavelets: the approximation) and one comprising the high frequencies (low scale) and the fast events (the detail) (Mallat 1989; Shiri 2018). In this research, the detail coefficients and approximation (A) sub-time series were computed through Equation (8). DWT has presented its capabilities in such kinds of studies by increasing the performance accuracy of the soft computing models through pre-processing the input variables (e.g. Shiri and Kisi 2010).

5. Coupled wavelet-MARS (WMARS) model

WMARS models were built through coupling the DWT and MARS techniques. The Daubechies (dbN) wavelet was used as mother wavelet, which is among the extensively applied wavelet functions in this type of studies since it is orthogonal discrete wavelet where the inverse wavelet transform is the adjoin wavelet transform (Kisi and Shiri 2012; Nourani et al. 2009). This type of mother wavelets does not have closed form and is represented numerically by some coefficients. In dbN, the N represents the vanishing moments, where higher N values lead to more localized and smooth filter, but also needs more coefficients to be represented, so db4 might be an optimum choice for signal analysis, although there is no fixed rule for selecting N number (Nourani and).

WMARS model is a MARS method that uses the sub-series of DWT that have been extracted from original time series. Hence, the original time series of stream flow (Q_W) and SSL records were decomposed into a certain number of sub-series (D_S) using the Mallat's algorithm (Mallat 1989). Then, the sub-series were used as inputs (with different lags, as mentioned before) of the MARS model to simulate SSL values. The number of decomposition level was determined through a logarithmic rule [log(n); n is the number of available patterns of each variable] as advised in literature (e.g. Shiri 2018). Accordingly, the number of decomposition levels was set as 4 levels given that there are about 10 years data at each location [3654 patterns (or Barbourville and Pineville) or 4015 patterns (for Dos Rios)]. Selection of the effective details and approximations subcomponents was carried out using the correlation analysis. So, the correlation values between the mentioned vectors and the target parameters were calculated and the most correlated vectors were selected as inputs of the coupled models.

6. Sediment rating curve (SRC)

A sediment rating curve relates the SSL/concentration to the stream flow discharge (Q_W) through a power relationship as (Sandy 1990):

$$SSL = aQ_W^b \tag{9}$$

Where, a and b are regression coefficients. The *a* coefficient represents the soil erodibility, while the *b* coefficient corresponds to the river-scouring power (Atieh et al. 2015).

7. Methodology

Selection of the necessary inputs for constructing the regression-based and artificial intelligence models is very important as the inclusion of redundant variables would increase the computational costs dramatically and might reduce the modelling overall performance accuracy. Among different input selection methods, a linear cross-correlation technique might be suitable for time series analysis when the aim is to seek proper time lags of the studied variables (Bowden et al. 2005). Kisi (2009) indicated that the examining statistical characteristics of the SSL data such as cross-, auto- and partial auto-correlation might be useful for identifying a unique input to the data-driven methods in estimation SSL process for a basin. Defining the input matrix was established in two steps: first, the cross correlations (CCF) between the SSL and water flow discharge (Q_W) values were analyzed for defining the proper time lags of Q_W to be included the input matrix. Then, the partial auto correlation functions (PACF) of SSL data were calculated and analyzed per studied station to identify the suitable SSL lags for inclusion in the input matrix. Figure 1 presents the CCFs and PACFs of SSL and Q_W data for the studied stations. From the figure, it is clear that three or four time lags of SSL records would be influential in modelling the future SSL records, so four time lags were selected to be included in the input matrix. Similarly, four Q_W lags were selected as input parameters for modelling future SSL values. Table 3 sums up the evaluated input configurations in the present study, which have been selected based on previous literature considering the correlation values. It should be however noted that the correlation technique has a linear basis, so other nonlinear techniques, e.g. average mutual information (AMI) might be used in further studies to fix the input parameters.

Once the input was defined, it was introduced to the suggested (single MARS, coupled wavelet-MARS and SRC) models to simulate the SSL values at i^{th} time step. A common procedure for establishing the applied models would be using two/three blocks compartment of data for training,

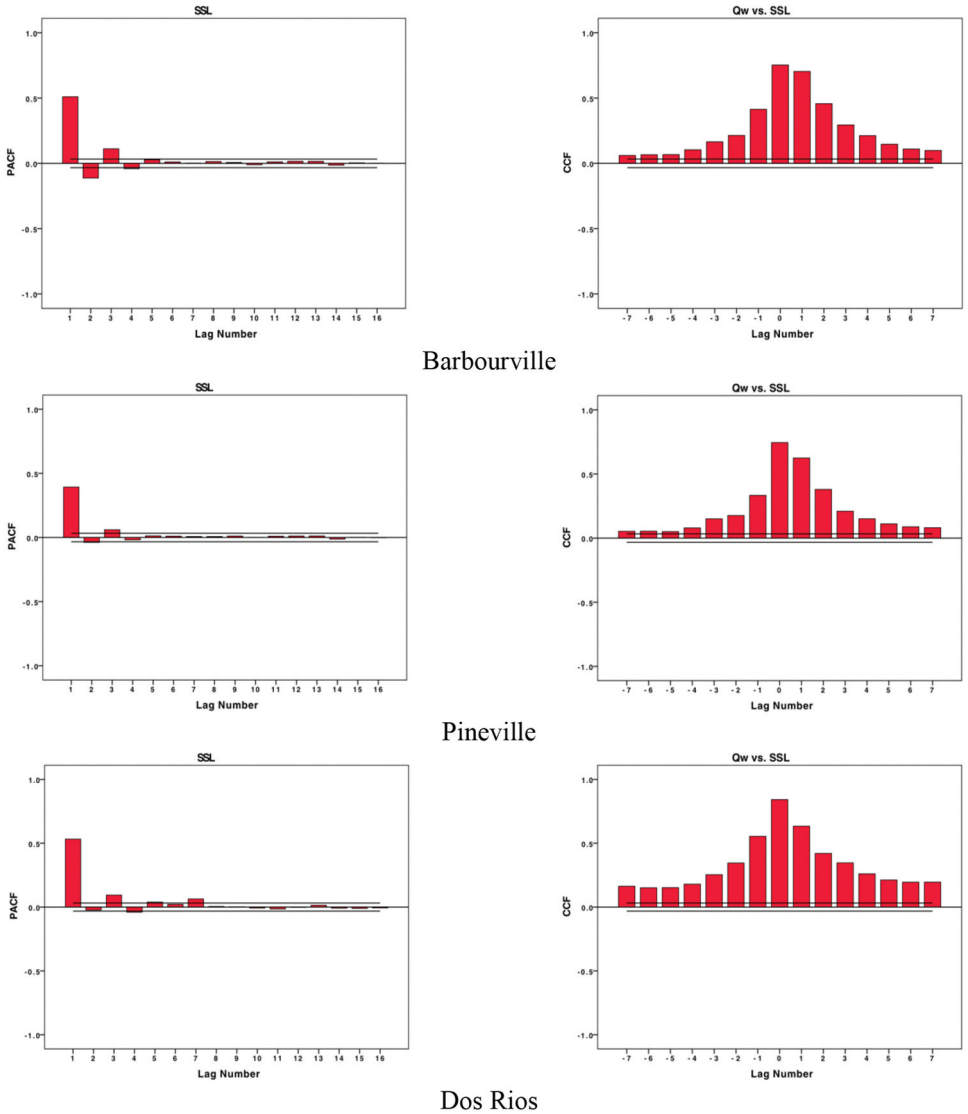

Figure 1. PACF and CCF diagrams of the SSL and SSL-Q_W records.

Table 3. Summary of the applied input configurations.

Model	Input variables
MARS1, WMARS1	Q_i, Q_{i-1}, Q_{i-2}, Q_{i-3}
MARS2, WMARS2	S_{i-1}, S_{i-2}, S_{i-3}, S_{i-4}
MARS3, WMARS3	S_{i-1}, Q_i, Q_{i-1}, Q_{i-2}, Q_{i-3}
MARS4, WMARS4	Q_i, Q_{i-1}, S_{i-1}, S_{i-2}
MARS5, WMARS5	Q_i, S_{i-1}

validating and testing the models. Although this seems a straightforward process for developing the models, a major drawback would be the partial scanning of the available patterns by the models and the conclusions obtained would be partially valid as the models have not been trained using all available patterns (that may have some extreme values). Therefore, a robust k-fold testing method was adopted in this study to evaluate the applied MARS and wavelet-MARS models. With using this data scanning method, the whole available patterns of SSL and Q_W are partitioned into 'k' blocks chronologically, and the models are trained each time using 'k-1' blocks and tested using the remaining one block. There is no fixed rule for defining the 'k' magnitudes in k-fold testing, but as the data comprise the time series of sediment and water discharge events during at least 10 years period, the minimum affordable test size was defined as 1 year (k = 1 year). Therefore, the patterns of 1 year were reserved as testing data each time and the models were trained using the remaining patterns. The process was repeated till all years participated in training-testing periods. Given that the total available time period was 31 years (for all three stations), total of 31 training-testing processes were carried out at each station per input combination for each model. So, total 465 processes (31 years*5 input combinations*3 models = 465 training-testing procedures) were performed in this study.

8. Performance evaluation criteria

Three statistical indices, viz., the coefficient of determination (r^2), the Nash-Sutcliffe coefficient (*NS*) and the variance accounted for (*VAF*) were utilized here for assessing the employed methodology as follows:

$$r^2 = \left(\frac{\sum_{i=1}^{n} \left(SSL_{io} - \overline{SSL_o}\right)\left(SSL_{iM} - \overline{SSL_M}\right)}{\sqrt{\sum_{i=1}^{n} \left(SSL_{io} - \overline{SSL_o}\right)^2 \sum_{i=1}^{n} \left(SSL_{iM} - \overline{SSL_M}\right)^2}} \right)^2 \quad (10)$$

$$NS = 1 - \frac{\sum_{i=1}^{n} \left(SSL_{io} - SSL_{iM}\right)^2}{\sum_{i=1}^{n} \left(SSL_{io} - \overline{SSL_o}\right)^2} \quad (11)$$

$$VAF = \left[1 - \frac{\mathrm{var}(SSL_{io} - SSL_{iM})}{\mathrm{var}(SSL_o)}\right] \times 100\% \quad (12)$$

In these equations, SSL_{io} represents the suspended sediment load value observed at the i^{th} time step and SSL_{iM} shows the corresponded predicted SSL value. *n* is the number of available patterns. $\overline{SSL_o}$ denotes the mean of the observational values and $\overline{SSL_M}$ stands for the mean value of the predictions. *NS* varies between 1 and $-\infty$, where *NS* = 1 shows the perfect fit between the observed and predicted values. The negative *NS* values generally show unacceptable model performance. *VAF* explains the portion of error variance in relation to the target variance and its perfect value is 100 (Tiyasha et al. 2020; Yaseen et al. 2019).

Given that the k-fold testing data management strategy has been adopted here, these indices were calculated for both the test stages (test years) and total study period. The values of the latter case were computed by making a global matrix of output-target values of all test stages for each input configuration and then, the statistical indices were computed.

9. Results and discussions

As mentioned, different input configurations were constructed (Table 3) to feed the applied models using the data from three stations. At the first part, different input configurations of Q_W and SSL records were introduced to the MARS model to predict the SSL values at the next prediction interval (single MARS models). In the second part, the wavelet decompositions of the same input parameters were utilized as input variables of the MARS model (hybrid wavelet-MARS models, WMARS), using the same input configurations. Table 4 sums up the global statistical indices of the applied models. The values correspond to the total study period of each station. Analyzing the values of the indices, some remarks might be highlighted. First, MARS3 and MARS4 models always gave the most accurate results among the other single models with the higher *NS* and r^2 values, although *VAF* values of these models were negative (unacceptable) in Pineville. The negative *VAF* values in this station represent that the variances of the models' errors are higher than those of the observed SSL records. Attending to the worst models, however, a general conclusion could not be achieved because MARS1, MARS2

Table 4. Global statistical indices of the applied models.

	Barbourville station			Dos Rios station			Pineville station		
	r^2	*NS*	*VAF*	r^2	*NS*	*VAF*	r^2	*NS*	*VAF*
Single models									
MARS1	0.855	0.362	−13.697	0.533	0.533	53.35	0.729	0.729	72.922
MARS 2	0.363	0.362	−13.697	0.362	0.362	36.264	0.231	0.231	13.913
MARS 3	0.878	0.877	26.717	0.826	0.826	82.643	0.810	0.810	−21.080
MARS 4	0.872	0.871	38.535	0.810	0.810	81.004	0.805	0.805	−13.903
MARS 5	0.670	0.670	67.050	0.331	0.331	33.165	0.638	0.638	63.859
Hybrid models									
WMARS 1	0.676	0.676	67.707	0.928	0.928	79.714	0.892	0.887	78.800
WMARS 2	0.739	0.735	74.732	0.799	0.774	69.994	0.660	0.659	61.541
WMARS 3	0.780	0.780	72.073	0.934	0.934	81.489	0.792	0.792	74.947
WMARS 4	0.657	0.649	64.931	0.934	0.934	79.181	0.751	0.748	68.333
WMARS 5	0.819	0.814	75.170	0.709	0.709	34.710	0.843	0.839	67.694
SRC	0.773	0.673		0.852	0.715		0.767	0.670	

and MARS5 presented the weakest performance accuracy in the Barbourville, Pineville and Dos Rios, respectively, with the lowest *NS* values. A possible reason for such differences might be the dissimilarities between the SSL-Q_W variation trends in the studied stations. Among three stations, the highest *NS* values of the MARS models were observed in Barbourville that showed the lowest skewness and C_V values of SSL records among the other stations. It should be however noted that, the values of both *NS* and *VAF* indices are high in Dos Rios Station with slight differences with the Barbourville indices. Next, coupling the wavelet with MARS model has improved the modelling accuracy. In the Barbourville Station, WMARS5 produced the most accurate results among the other applied input configuration. Although its *NS* value seems to be lower than those of the single MARS3 and MARS4 models (7% and 6% reduction in *NS* values with respect to MARS3 and MARS4, respectively), the *VAF* has been improved to great extent (65% and 48% increase in *VAF* with respect to the same models). In the Pineville Station, where the *VAF* values of MARS3 and MARS4 models were completely unacceptable (negative), WMARS1 gave the best performance among others. It improved the *NS* values of the best single MARS models through increasing the *NS* values by 9% and 10%, respectively. Improving the *VAF* values was very significant (78.80 for WMARS1 and negative values for single MARS models). In case of the Dos Rios Station, again, WMARS3 and WMARS4 gave the best performance accuracy with the highest NS and *VAF* among others. Their improvements in term of *NS* were also significant as can be seen from Table 4. It is relevant to note here that some inconsistencies that are observed between *NS* and *VAF* trends in different models might be linked to the theoretical background of these indices, where *VAF* focuses purely on the variance changes, while *NS* considers both the error and variance terms, simultaneously. Though each of them can be interpreted from their own viewpoints, *NS* benefitted from considering both the mentioned terms, so it would be better index for final judgement between the models and input configurations. Finally, comparing between stations of the hybrid models, it is seen that the highest *NS* values correspond to the Dos Rios Station, while its SSL records have presented the highest C_V and skewness values among others. A preliminary hypothesis with such situation would be difficulties bearing from high C_V and skewness values in extrapolating the target parameter magnitudes. Although this was the case in this station, hybrid models have had capability to handle such difficult extrapolation issue with high level of accuracy.

Figure 2 displays the observed and simulated SSL values of the best hybrid models in the studied stations. From the figure it is clear that the hybrid models have had good capability in simulating higher SSL values in all three stations, although some deviations between observed-simulated values can be seen for lower SSL records. Keeping in mind such differences, the models gave promising results because it is very important to estimate higher SSL values. The main reason of the low accuracy of the hybrid MARS model in estimating low SSL records is the calibration of this model is done by minimizing the square error (SE). This error is highly sensitive to peak SSL values.

Further, a breakdown of the statistical indices values per test stages for the hybrid and SRC models were carried out to analyze the temporal variations of the models' performance accuracy during the test stages. Figure 3 presents the *NS* variations per test stage of each station for these models. First, obvious variations of *NS* values can be detected among the test stages (years) for all the stations. Differences between the maximum and minimum *NS* values (ΔNS) of the best models for Barbourville, Pineville and Dos Rios stations were 0.430 (WMARS5), 0.433 (WMARS1) and 0.432 (WMARS3), respectively. On the other hand, maximum ΔNS values were observed for WMARS2 (0.707 and 0.905 in Barbourville and Pineville, respectively) and WMARS5 (0.673 in Dos Rios). Moreover, ΔNS values of the SRC model were considerably high in all the stations: 0.600, 0.506 and 0.655 for Barbourville, Pineville and Dos Rios. Second, analysis per station variations of the *NS* values

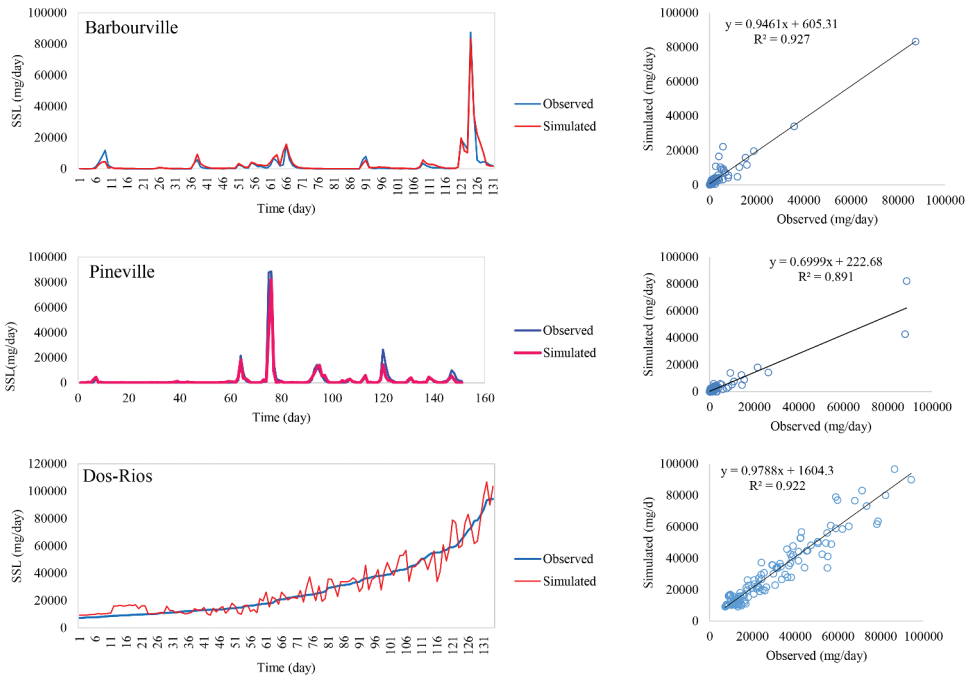

Figure 2. Observed vs. simulated SSL values of the best hybrid model in studied stations for some limited time periods.

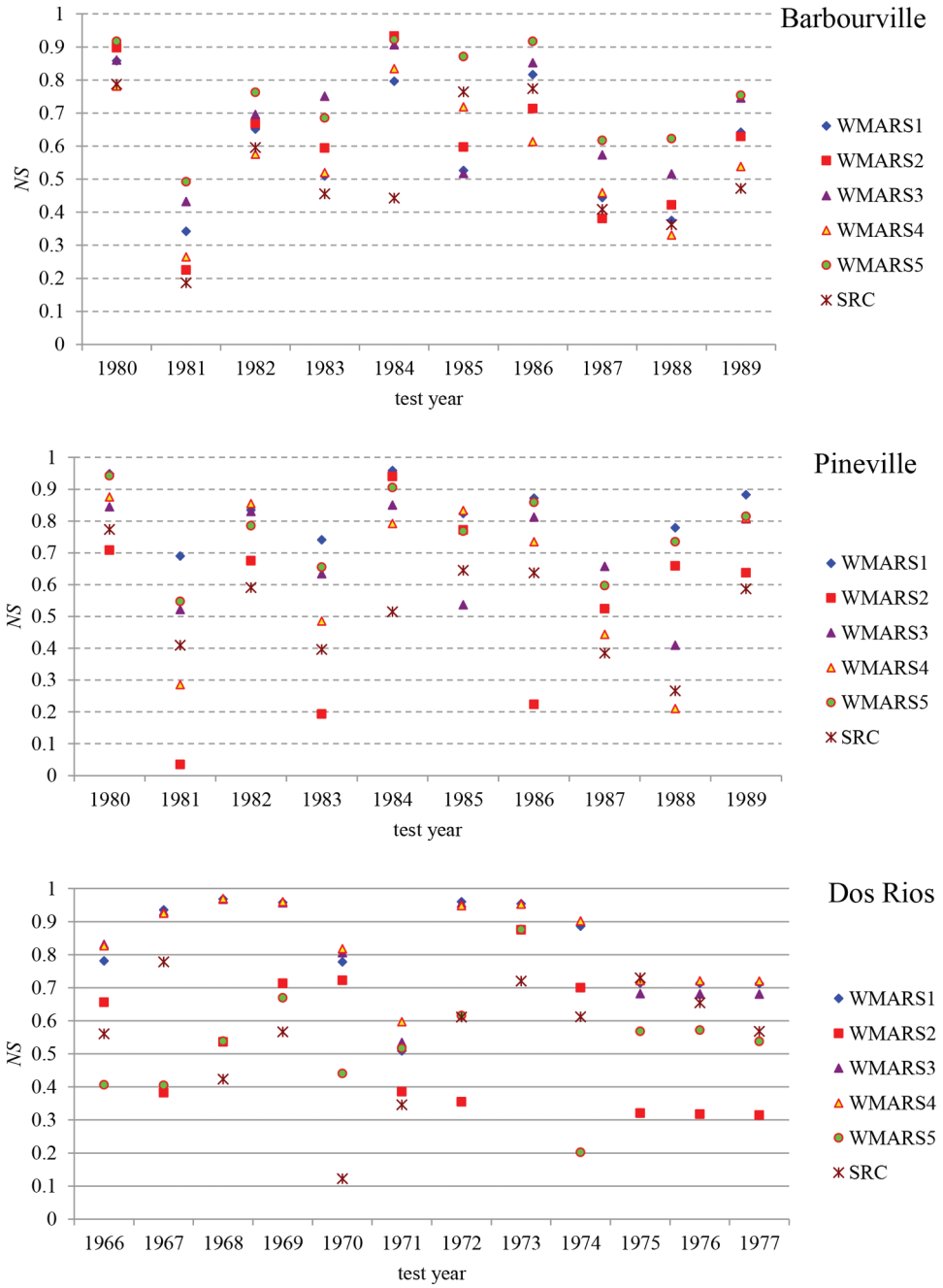

Figure3. Temporal variations of the *NS* values among the test stages (years)

Figure 3. Temporal variations of the *NS* values among the test stages (years).

showed that all the models gave lower *NS* values for the test year 1981 in Barbourville, while they gave higher *NS* values for 1984 (except SRC). One possible reason of this behaviour might be the statistical characteristics (e.g. C_V, skewness, etc) of the utilized data during the studied years. Although these characteristics are similar for Q_W (flow discharge) values over the years, considerable differences (not presented here) were observed for SSL records. Analyzing those values showed that SSL presented the highest C_V values for the test year 1984 (6.480) with respect to the rest of the years and the total study period that could make the simulation difficult. So, such variations cannot be explained by these indices and other possible reasons, e.g. hysteresis effect should be considered. Analysis of the Q_W-SSL plots per test year (Figure 4) revealed that there are lots of loops in Q_W-SSL relations for the test year 1981 in Barbourville that might make the SSL simulations difficult using Q_W records. Attending to the Pineville and Dos Rios sites, the *NS* values monotonously fluctuated among the test years, and the best models (based on Table 4 indices) always gave the highest *NS* values in relation to the other models in all test stages.

Summarizing, it might be stated that coupling wavelet with MARS is a promising approach for predicting suspended sediment load of rivers, although adopting a proper data management scenario is of crucial importance in this regard. The outcomes of the present study revealed remarkably the necessity of a complete data scan procedure to achieve the most reliable simulations of SSL records, especially when hysteresis phenomenon is a dominant hydrologic behaviour of the studied rivers.

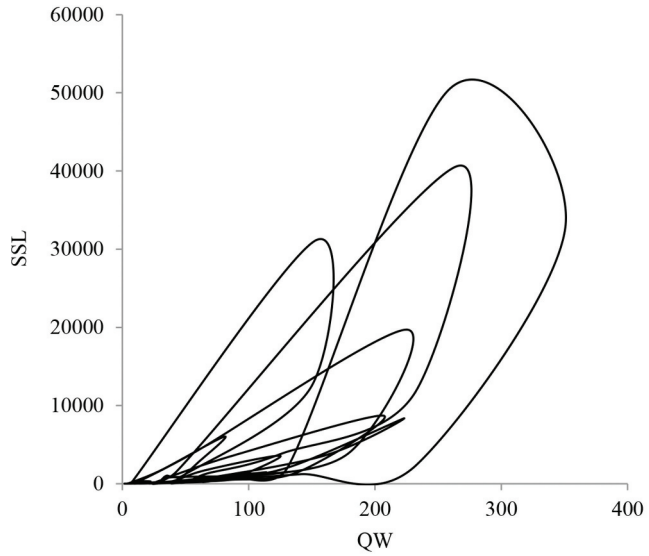

a) QW-SSL relations (Hysteresis effect)

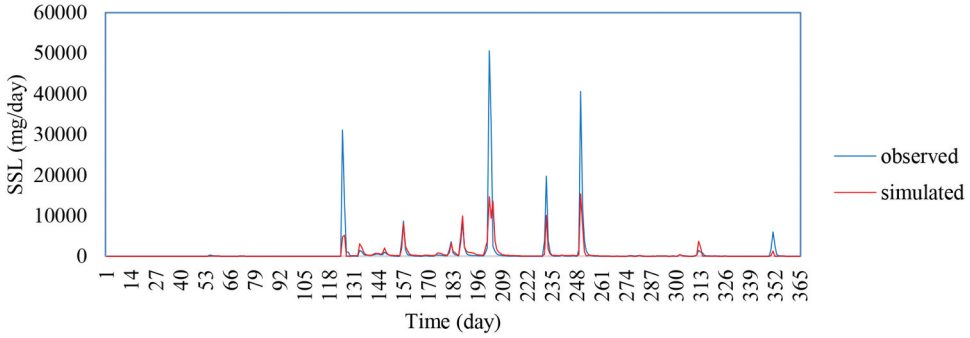

b) Observed vs. simulated values of SSL values

Figure 4. Hysteresis effect and observed-simulated values for Barbourville station during the test year 1981.

10. Conclusions

A new hybrid wavelet-based processed signals and multi adaptive regression spline (WMARS) methodology was proposed in the present study for hydrological modelling of suspended sediment load (SSL) values using historical records of three rivers in USA. The stations covered wide range of SSL variations in their time series. Various input configurations were constructed based on the statistical characteristics of the SSL and stream flow (Q_W) records to be applied by the models. A comparison was also made between the hybrid models and single MARS and traditional sediment rating curves (SRC) approached. All the applied models were assessed by a powerful k-fold testing data management strategy to get the clearest information on modelling performance accuracy during the available chronologic period. The obtained results revealed that using both SSL and Q_W records as model inputs simultaneously is necessary for better mapping the relations between the antecedent and future SSL values. Nonetheless, strengthening the MARS models by wavelet transform outcomes has considerably improved the modelling accuracy. Further, adoption of a complete data scanning procedure, e.g. k-fold testing is necessary in such kinds of studies to avoid overfitting and other model development-based problems. The present paper used data from 3 stations of USA. Further studies might be needed using more data and other hybrid models to improve the outcomes. Moreover, event-based stream flow and SSL records might be utilized for better describing the downscaled SSL variations and hysteresis effect implications.

Disclosure statement

No potential conflict of interest was reported by the authors.

References

Adamowski, J., Chan, H.F., Prasher, S.O., and Sharda, V.N. (2012). "Comparison of multivariate adaptive regression splines with coupled wavelet transform artificial neural networks for runoff forecasting in Himalayan micro-watersheds with limited data." *J. Hydroinf.*, 14(3), 731–744.

Adamowski, J., and Sun, K. (2010). "Development of a coupled wavelet transform and neural network method for flow forecasting of non-perennial rivers in semi-arid watersheds." *J. Hydrol.*, 390, 85–91.

Andres, J.D., Lorca, P., de Cos Juez, F.J., and Sánchez-Lasheras, F. (2010). "Bankruptcy forecasting: A hybrid approach using Fuzzy c-means clustering and Multivariate Adaptive Regression Splines (MARS)." *Expert. Syst. Appl.*, 38, 1866–1875.

Atieh, M., Mehltretter, S.L., Gharabaghi, B., and Rudra, R. (2015). "Integrative neural networks model for prediction of sediment rating curve parameters for ungauged basins." *J. Hydrol.*, 531, 1095–1107.

Aytek, A., and Kisi, O. (2008). "A genetic programming approach to suspended sediment modeling." *J. Hydrol.*, 351, 288–298.

Bisoyi, N., Gupta, H., Padhy, N.P., and Chakrapani, G.J. (2019). "Prediction of daily sediment discharge using a back propagation neural network training algorithm: A case study of the Narmada River." *Int. J. Sediment Res*, 34(2), 125–135.

Bogardi, J. (1974). *Sediment transport in alluvial streams*. Akademiai Kiado, Budapest Hungary, 486.

Bowden, G.J., Maier, H.R., and Dandy, G.C. (2005). "Input determination for neural network models in water resources applications. Part1- Background and methodologies." *J. Hydrol.*, 301, 75–92.

Friedman, J.H. (1991). "Multivariate adaptive regression splines." *Ann. Stat.*, 19, 1.

Ghose, D.K., and Samantaray, S. (2018). "Modelling sediment concentration using back propagation neural network and regression coupled with genetic algorithm." *Procedia Comput Sci*, 125, 85–92.

Goyal, M.K. (2014). "Modeling of sediment yield prediction using M5 model tree algorithm and wavelet regression." *Water Resour. Manage.*, 28(7), 1991–2003.

Graf, R., Zhu, S., and Sivakumar, B. (2019). "Forecasting river water temperature time series using a wavelet–neural network hybrid modelling approach." *J. Hydrol.*, 578, 124115.

Himanshu, S.K., Pandey, A., and Yadav, B. (2017). "Ensemble wavelet-support vector machine approach for prediction of suspended sediment load using hydrometeorological data." *J. Hydrol. Eng*, 22, 7.

Homaei, F., and Najafzadeh, M. (2020). "A reliability-based probabilistic evaluation of the wave-induced scour depth around marine structure piles." *Ocean Eng.*, 196, 106818.

Karim, M.F., and Kennedy, J.F. (1990). "Menu of coupled velocity and sediment-discharge relations for rivers." *J. Hydraul. Eng. ASCE*, 116 (8), 978–996.

Khosravi, K., Mao, L., Kisi, O., Yaseen, Z.M., and Shahid, S. (2018). "Quantifying hourly suspended sediment load using data mining models: Case study of a glacierized Andean catchment in Chile." *J. Hydrol.*, 567, 165–179.

Kisi, O. (2009). "Neural networks and wavelet conjunction model for in- termittent stream flow forecasting." *J. Hydrol. Eng.*, 14(8), 773–782.

Kisi, O. (2011). "Evapotranspiration modeling using a wavelet regression model." *Irrig. Sci.*, 29, 241–252.

Kisi, O., Hossein Zadeh Dalir, A., Cimen, M., and Shiri, J. (2012). "Suspended sediment modeling using genetic programming and soft computing techniques." *J. Hydrol.*, 450–451, 48–58.

Kisi, O., and Shiri, J. (2011). "Precipitation forecasting using wavelet-genetic programming and wavelet-neuro-fuzzy conjunction models." *Water Resour. Manage.*, 25(13), 3135–3152.

Kisi, O., and Shiri, J. (2012). "River suspended sediment estimation by climatic variables implication: Comparative study among soft computing techniques." *Comput. Geosci.*, 43, 73–82.

Kisi, O., and Yaseen, Z.M. (2019). "The potential of hybrid evolutionary fuzzy intelligence model for suspended sediment concentration prediction." *Catena*, 174, 11–23.

Liu, Q.J., Zhang, H.Y., Gao, K.T., Xu, B., Wu., J.Z., and Fang, N.F. (2019). "Time-frequency analysis and simulation of the watershed suspended sediment concentration based on the Hilbert-Huang transform (HHT) and artificial neural network (ANN) methods: A case study in the Loess Plateau of China." *Catena*, 179, 107–118.

Londhe, S., and Narkhdehe, S. (2018). "Forecasting stream flow using hybrid neuro-wavelet technique." *ISH J. Hydraul. Eng.*, 24(3), 275–284.

Lopes, V.L., and Ffolliott, P.F. (1993). "Sediment rating curves for a clearcut Ponderosa Pine watershed in northern Arizona." *Water Resour. Bull.*, 29(3), 369–382.

Makarynskyy, O., Makarynska, D., Rayson, M., and Langtry, S. (2015). "Combining deterministic modelling with artificial neural networks for suspended sediment estimates." *Appl. Soft. Comput.*, 35, 247–256.

Mallat, S.G. (1989). "A theory for multi resolution signal decomposition: The wavelet representation." *IEEE Trans. Pattern Anal. Mach. Intell.*, 11(7), 674–693.

McBean, E., and Al-Nassri, S. (1988). "Uncertainty in suspended sediment transport curves." *J. Hydraul. Eng.*, 114, 63–74.

Najafzadeh, M. (2020). "Evaluation of conjugate depths of hydraulic jump in circular pipes using evolutionary computing." *Soft Comput.*, 23, 13375–13391.

Najafzadeh, M., and Kargar, A.R. (2019). "Gene-expression programming, evolutionary polynomial regression, and model tree to evaluate local scour depth at culvert outlets." *J. Pipeline Syst. Eng. Pract.*, 10, 3. doi: 10.1061/(ASCE)PS.1949-1204.0000376.

Najafzadeh, M., and Oliveto, G. (2020). "Riprap incipient motion for overtopping flows with machine learning models." *J. Hydroinf.*, doi: 10.2166/hydro.2020.129.

Nazafzadeh, M., and Zeinolabedini, M. (2018). "Derivation of optimal equations for prediction of sewage sludge quantity using wavelet conjunction models: An environmental assessment." *Environ. Sci. Pollut. Res.*, 25, 22931–22943.

Nourani, V., Alami, M.T., and Aminfar, M.H. (2009). "A combined neural-wavelet model for prediction of Ligvanchai watershed precipitation." *Eng. Appl. Artif. Intell.*, 22(3), 466–472.

Nourani, V., Hosseini, A., Adamowski, J., and Kisi, O. (2014). "Applications of hybrid wavelet–Artificial Intelligence models in hydrology: A review." J. Hydrol., 514, 358–377

Nourani, V., Kisi, O., and Komasi, M. (2011). "Two hybrid artificial intelligence approaches for modeling rainfall–runoff process." *J. Hydrol.*, 402, 41–59.

Nourani, V., Molaju, A., Davanlou Tajbaksh, A., and Najafi, H. (2019). "A wavelet based data miningt for suspended sediment load modeling." *Water Resour.Manage.*, 33(5), 1769–1784.

Partal, T., and Cigizoglu, H.K. (2008). "Estimation and forecasting of daily suspended sediment data using wavelet-neural networks." *J. Hydrol.*, 358(3–4), 317–331.

Partal, T., and Kisi, O. (2007). "Wavelet and neuro fuzzy conjunction model for precipitation forecasting." *J. Hydrol.*, 342, 199–212.

Peng, T., Zhou, J., Zhang, C., and Fu, W. (2017). "Streamflow forecasting using empirical wa- velet transform and artificial neural networks." *Water*, 9(6), 406.

Rajaee, T. (2010). "Wavelet and neuro-fuzzy conjunction approach for suspended sediment prediction." *Clean-Soil Air Water*, 38, 275–288.

Rajaee, T. (2011). "Wavelet and ANN combination model for prediction of daily suspended sediment load in rivers." *Sci. Total Environ.*, 409, 2917–2928.

Rajaee, T., Nourani, V., Zounematkermani, M., and Kisi, O. (2011). "River suspended sediment load prediction: Application of ANN and wavelet conjunction model." *J. Hydrol. Eng.*, 16(8), 613–627.

Sadeghi, G., Najafzadeh, M., and Ameri, M. (2020). "Thermal characteristics of evacuated tube solar collectors with coil inside: An experimental study and evolutionary algorithms." *Renewable Energy*, 151, 575–588.

Salih, S.Q., Sharafati, S.Q., Khosravi, K., Faris, H., Kisi, O., Tao, H., Ali, M., and Yaseen, Z.M. (2020). "River suspended sediment load prediction based on river discharge information: Application of newly developed data mining models." *J. Hydraul. Eng.*, 65(4), 624–637.

Samantaray, S., and Ghose, D.K. (2018). "Evaluation of suspended sediment concentration using descent neural networks." *Procedia Comput. Sci.*, 132, 1824–1831.

Sandy, R. (1990). *Statistics for business and economics*. McGraw-Hill Publishing, New York, 1117

Seo, Y., Kim, S., Kisi, O., Singh, V.P., and Parasuraman, K. (2016). "River stage forecasting using wavelet packet decomposition and machine learning models." *Water Resour. Manage.*, 30(11), 1–25.

Sharda, V., Prasher, S.O., Patel, R.M., Ojavasi, P.R., and Prakash, C. (2006). "Modeling runoff from middle Himalayan watersheds employing artificial intelligence techniques." *Agric. Water Manage.*, 83, 233–242.

Shiri, J. (2018). "Improving the performance of the mass transfer-based reference evapotranspiration estimation approaches through a coupled wavelet-random forest methodology." *J. Hydrol.*, 561, 737–750.

Shiri, J. (2019). "Prediction vs. estimation of dewpoint temperature: Assessing GEP. MARS and RF models." *Hydrol. Res.*, 50(2), 633–643.

Shiri, J., and Kisi, O. (2010). "Short-term and long-term streamflow forecasting using a wavelet and neuro-fuzzy conjunction model." *J. Hydrol.*, 394(3–4), 486–493.

Shiri, J., and Kisi, O. (2012). "Estimation of daily suspended sediment load by using wavelet conjunction models." *ASCE J. Hydrol. Eng.*, 17 (9), 986–1000.

Sivakumar, B. (2006). "Suspended sediment load estimation and the problem of inadequate data sampling: A fractal view." *Earth Surf. Proc. Land.*, 31, 414–427.

Tao, H., Keshtegar, B., and Yaseen, Z.M. (2019). "The feasibility of integrative radial basis M5Tree predictive model for river suspended sediment Load simulation." *Water Resour.Manage.*, 33, 4471–4490.

Tiyasha, T., Tung, T.M., and Yaseen, Z.M. (2020). "A survey on river water quality modelling using artificial intelligence models: 2000–2020." *J. Hydrol.*, 585, 124670.

Vanoni, V.A. (1971). "Sediment discharge formulas." *J. Hydraul. Div. ASCE*, 97(4), 523–567.

Wang, W., Jin, J., and Li, Y. (2009). "Prediction of inflow at three Gorges dam in Yangtze River with wavelet network model." *Water Resour. Manage.*, 23(13), 2791–2803.

Yaseen, Z.M., Sulaiman, S.O., Deo, R.C., and Chau, K.W. (2019). "An enhanced extreme learning machine model for river flow forecasting: State-of-the-art, practical applications in water resource engineering area and future research direction." *J. Hydrol.*, 569, 387–408.

Zeinolabedini, M., and Najafzadeh, M. (2019). "Comparative study of different wavelet-based neural network models to predict sewage sludge quantity in wastewater treatment plant." *Environ. Monit. Assess.*, 191(2019), 163.

Zhang, J., Zhang, X., Niu, J., Hu, B.X., Soltanian, M.R., Qiu, H., and Yang, L. (2019). "Prediction of groundwater level in seashore reclaimed land using wavelet and artificial neural network-based hybrid model." *J. Hydrol.*, 577, 123948.